The zinc finger transcriptional repressor Blimp1/Prdm1 is dispensable for early axis formation but is required for specification of primordial germ cells in the mouse

Stéphane D. Vincent[1,*], N. Ray Dunn[1,†], Roger Sciammas[3,‡], Miriam Shapiro-Shalef[4], Mark M. Davis[3], Kathryn Calame[4], Elizabeth K. Bikoff[1,2,§,¶] and Elizabeth J. Robertson[1,2,§,¶]

[1]Department of Molecular and Cellular Biology, Harvard University, Cambridge, MA 02138, USA
[2]Wellcome Trust Center for Human Genetics, University of Oxford, Oxford OX3 7BN, UK
[3]Department of Microbiology and Immunology, Stanford University School of Medicine, Stanford, CA 94305, USA
[4]Department of Microbiology, Columbia University College of Physicians and Surgeons, New York, NY 10032, USA
*Present address: Institut Pasteur, Department of Developmental Biology, 25 Rue du Dr Roux, Paris, France
†Present address: ES Cell International, Singapore
‡Present address: Department of Molecular Genetics and Cell Biology, University of Chicago, Chicago, IL, USA
§Joint senior authors
¶Authors for correspondence (e-mail: Elizabeth.Bikoff@well.ox.ac.uk or Elizabeth.Robertson@well.ox.ac.uk)

Accepted 14 January 2005

Development 132, 1315-1325
Published by The Company of Biologists 2005
doi:10.1242/dev.01711

Summary

Blimp1, a zinc-finger containing DNA-binding transcriptional repressor, functions as a master regulator of B cell terminal differentiation. Considerable evidence suggests that *Blimp1* is required for the establishment of anteroposterior axis formation and the formation of head structures during early vertebrate development. In mouse embryos, *Blimp1* is strongly expressed in axial mesendoderm, the tissue known to provide anterior patterning signals during gastrulation. Here, we describe for the first time the defects caused by loss of *Blimp1* function in the mouse. *Blimp1* deficient embryos die at mid-gestation, but surprisingly early axis formation, anterior patterning and neural crest formation proceed normally. Rather, loss of *Blimp1* expression disrupts morphogenesis of the caudal branchial arches and leads to a failure to correctly elaborate the labyrinthine layer of the placenta. *Blimp1* mutant embryos also show widespread blood leakage and tissue apoptosis, and, strikingly, *Blimp1* homozygous mutants entirely lack PGCs. At the time of PGC allocation around 7.25 days post coitum, *Blimp1* heterozygous embryos exhibit decreased numbers of PCGs. Thus *Blimp1* probably acts to turn off the default pathway that allows epiblast cells to adopt a somatic cell fate, and shifts the transcriptional program so that they become exclusively allocated into the germ cell lineage.

Key words: Blimp1/Prdm1 (Blimp-1), Mouse, Branchial arches, Vasculature, Primordial germ cells

Introduction

Current models suggest that programmed cell growth and differentiation during development are controlled by master regulatory genes that coordinate the activities of cell-type-specific transcription factors. However, relatively few examples of such regulators with proven capabilities to govern global patterns of gene expression have been described in the literature. *Blimp1* (*Prdm1* – Mouse Genome Informatics), a Krüppel-type zinc-finger-containing DNA-binding transcriptional repressor originally cloned by its ability to bind the human β-IFN promoter (Keller and Maniatis, 1991), was also independently identified due to its cell-type-specific expression in murine plasmacytoma cell lines (Turner et al., 1994). *Blimp1* expression is dramatically upregulated coincident with plasma cell differentiation, and enforced expression is sufficient to drive B cells to become antibody-secreting cells (reviewed by Calame et al., 2003). Recent studies have shown that *Blimp1* plays an essential role in B-cell development (Shapiro-Shelef et al., 2003). Thus conditional inactivation of *Blimp1* in B cells disrupts their terminal differentiation to plasma cells, and consequently serum Ig levels are markedly reduced. *Blimp1* has been shown to repress expression of cell cycle regulators such as *Myc*, p18 and p21 (Sciammas and Davis, 2004; Shaffer et al., 2002; Yu et al., 2000), and consequently *Blimp1*-deficient B cells display a hyperproliferative phenotype (Shapiro-Shelef et al., 2003). *Blimp1* downregulates the expression of transcription factors such as CIITA and Pax5, which are essential for B-cell antigen presentation and receptor signaling (Lin et al., 2002; Piskurich et al., 2000). *Blimp1* has also been implicated as a master regulator of myeloid cell terminal differentiation (Chang et al., 2000).

Considerable evidence suggests that *Blimp1* acts to control anteroposterior axis formation and development of the head structures in early vertebrate embryos. In *Xenopus* and zebrafish, *Blimp1* transcripts localize to the signaling centers that pattern the forebrain, namely the leading anterior mesendoderm and prechordal plate (Baxendale et al., 2004; de Souza et al., 1999). Overexpression of *Blimp1* in *Xenopus* embryos downregulates *Xbra* and *Myf5* activities, which are

required for formation of trunk mesoderm, and consequently causes axis truncations. *Blimp1* also activates anterior mesendodermal markers such as *goosecoid* and *cerberus* in animal cap explant assays (de Souza et al., 1999). Similarly, zebrafish embryos treated with *Blimp1* antisense morpholino oligonucleotides show loss of anterior structures and display a foreshortened body axis (Baxendale et al., 2004). The analogous anterior signaling centers in mouse, namely the anterior visceral endoderm (AVE) and anterior definitive endoderm (ADE)/prechordal plate, have been shown to express *Blimp1* transcripts (de Souza et al., 1999). Thus it has been widely assumed that *Blimp1* also plays a crucial role in anterior patterning during mammalian development.

Blimp1 activity is also required for lineage specification in two additional tissues in zebrafish. A hypomorphic allele of the *Blimp1* ortholog *u-boot* (*ubo*) results in viable animals lacking slow-twitch muscle fibers (Baxendale et al., 2004; Roy et al., 2001). Molecular analysis reveals muscle precursors fail to differentiate into slow-twitch fibers in response to Hh. *ubo* activates expression of the slow myosin heavy chain, and represses expression of the fast myosin heavy chain. Interestingly, *ubo* also acts downstream of BMP signaling in specification of the trunk and cranial neural crest precursors (Roy and Ng, 2004). Whether *Blimp1* similarly controls muscle development and/or formation of neural crest derivatives in the mammalian embryo remains unknown.

Here, we describe for the first time the defects caused by *Blimp1* loss of function in the mouse. *Blimp1*-deficient embryos die at mid-gestation, but surprisingly early axis formation, anterior patterning and neural crest formation proceed normally. Rather loss of *Blimp1* expression disrupts morphogenesis of the caudal branchial arches and leads to a failure to correctly elaborate the labyrinthine layer of the placenta. *Blimp1* mutant embryos also show widespread blood leakage and tissue apoptosis. *Blimp1* transcripts are first detectable in the visceral endoderm overlying the proximal epiblast prior to gastrulation, and within the epiblast are restricted to the primordial germ cells (PGCs) at the time they first appear in the posterior allantois. *Blimp1* expression persists as PGCs migrate anteriorly toward the genital ridges (Chang and Calame, 2002). Strikingly, we report here that *Blimp1* homozygous mutants entirely lack PGCs. Quantitative analysis of PGC numbers at sequential embryonic stages reveals that this loss occurs at the time of their allocation around 7.25 days post coitum (dpc). Moreover *Blimp1* heterozygous embryos exhibit a dose-dependent decrease in PGC numbers. The present experiments thus identify *Blimp1* as the first transcriptional regulator required for establishment of the mammalian germ line.

Materials and methods

Generation of *Blimp1* mutant alleles

We engineered two independent mutations at the *Prdm1*/*Blimp1* locus. The homology arms were subcloned into the vector described previously that contains *Lox*P-flanked *pgk-hygro*, and *hsv-tk* and *pgk-dta* negative-selection cassettes (Vincent et al., 2004). As shown in Fig. 2, the BAH construct contains 3.7-kb (*Xba*I-*Apa*I) 5′ and 3.7-kb (*Pst*I-*Msc*I) 3′ homology arms, and deletes 3 kb spanning the promoter and exons 1 to 3, whereas the BEH vector, containing 4.8-kb (*Xba*I-*Eag*I) 5′ and 3.7-kb (*Pst*I-*Msc*I) 3′ homology arms, creates a smaller deletion beginning upstream of the ATG in exon 1 and including exon 3. Linearized vectors were electroporated into CCE ES cells. Drug-resistant colonies were screened by Southern blot analysis using a 5′ external probe (*Sal*I-*Spe*I). Both vectors gave a targeting frequency of approximately 3%. Candidate targeted clones were expanded and re-screened using a 3′ external probe (*Msc*I-*Nco*I). For each construct, three correctly targeted ES clones were injected into C57BL/6J blastocysts to generate germ line chimeras. To excise the *hygro* selection cassette, *prdm1*^{BAH} and *prdm1*^{BEH} germ-line male chimeras were mated with *Sox2Cre* transgenic females that express *Cre* in the germ line (Vincent and Robertson, 2003), yielding the so-termed *prdm1*^{BA} and *prdm1*^{BE} derivative alleles, respectively. The removal of the selection cassette did not affect the phenotype.

Mouse strains and genotyping procedures

The *prdm1*^{BAH} and *prdm1*^{BEH} mutant strains were maintained on a C57BL/6×129/Sv//Ev background, whereas *prdm1*^{BA} and *prdm1*^{BE} mutations were outcrossed to ICR. Primers ApaMUT– (5′-CGA AGT TAT GGA TCA TCA AGG-3′) and ApaCOM+ (5′-TGT ATG CCC CGT GTG TTT AG-3′) that amplify a 259-bp band were used to detect the *prdm1*^{BA} and *prdm1*^{BAH} alleles. The *prdm1*^{BE} and *prdm1*^{BEH} alleles were detected using primers EagMUT– (5′-ATT ATA CGA AGT TAT GGA TCA TC-3′) and EagCOM+ (5′-TTG GTA AAG AAG TCT GCG GC-3′) that amplify a 188-bp band. Primers EagCOM+ and EagWT– (5′-TCG TAC CCA CAC GTT TTT CC-3′) were used to detect a 307-bp band corresponding to the wild-type allele. The *prdm1*^{CD} strain was maintained on an albino outbred ICR background and genotyped as described (Shapiro-Shelef et al., 2003). Embryos were individually genotyped prior to histological analysis, whole-mount in situ hybridization and primordial germ-cell staining.

Whole-mount in situ hybridization and histology

Whole-mount in situ hybridization was performed according to standard protocols (Nagy et al., 2003). Two *Blimp1*/*Prdm1* probes were used. The first was derived from the EST mB3 (IMAGE clone 1165721) specific for the 3′UTR, and the second, generated by PCR, was specific for exons 4 and 5. No expression pattern differences were observed between these two probes. *Fgf8*, *Crabp1*, *Shh*, *Hoxb1* and *Evx1* probes have been described previously (Dolle et al., 1989; Vincent et al., 2003). India ink was injected into the outflow tract of freshly isolated 9.5 dpc embryos to visualize the major arteries. For histological analysis, embryos fixed in 4% paraformaldehyde, were dehydrated through an ethanol series, and embedded in wax before sectioning. Hematoxylin and Eosin staining was performed according to standard protocols.

Alkaline phosphatase staining and SSEA1 immunostaining

Embryos were dissected from the decidua and Reichert's membrane. Pieces of the extraembryonic tissue (7.75-8.5 dpc embryos) or yolk sac (9.5 dpc embryos) were kept for genotyping. Alkaline phosphatase staining was performed as described previously (Labosky and Hogan, 1999; Lawson et al., 1999). SSEA1 immunostaining was performed as previously described (Gomperts et al., 1994).

Statistics

Regression analysis and comparison of regression lines were performed using the F test to compare variances (Snedecor and Cochran, 1967).

Results

Generation of Blimp1 loss-of-function mutants

Considerable evidence suggests that *Blimp1* plays a crucial role as a master regulator during axis formation and anterior patterning in vertebrate embryos (de Souza et al., 1999).

Consistent with this suggestion, in mouse embryos *Blimp1* transcripts are strongly expressed in the anterior region in the prechordal plate, as well as in the anterior definitive endoderm (de Souza et al., 1999). Immunohistochemical experiments have also described expression at later stages in the primordial germ cells and gut endoderm (Chang and Calame, 2002). To assess *Blimp1* expression from pre-gastrulation stages onwards, we performed WISH analysis. *Blimp1* transcripts are initially detected at day 6.0 post coitum (dpc) in the visceral endoderm overlying the proximal epiblast (Fig. 1A), and by 7.5 dpc are confined to the anterior mesendoderm (Fig. 1D,E) (de Souza et al., 1999) and the PGCs (Fig. 1B-F). We have previously shown that during gastrulation Nodal signals are required to specify derivatives of the anterior primitive streak, including the anterior mesendoderm (Vincent et al., 2003), raising the interesting possibility that *Blimp1* might potentially function as a transcriptional regulator downstream of the Nodal signaling pathway.

To learn more about possibly conserved *Blimp1* functions in axis formation and anterior patterning, we generated two independent mutations designated *prdm1*^{BEH} and *prdm1*^{BAH}. Both alleles delete 5′ regions of the *Blimp1* locus, including the first three coding exons (see Materials and methods; Fig. 2). Heterozygous mice carrying these mutations are healthy and fertile. However, intercross matings produced no live born homozygous offspring (see Table 1). Mutant embryos were recovered at the expected Mendelian ratio up to 9.5 dpc, but became hemorrhagic and were dying one day later. Homozygous mutant embryos failed to survive beyond 10.5 dpc.

The *prdm1*^{CD} mutation eliminates exons 6-8, encoding the five zinc fingers crucial for DNA binding, and disrupts Blimp1 protein expression as assessed by western blot analysis (Shapiro-Shelef et al., 2003). To compare the mutant phenotypes, *prdm1*^{CD} heterozygotes were intercrossed, and embryos collected between 9.5 and 11.5 dpc. We observed exactly the same range of tissue defects as described in detail below. Finally, when mice carrying the *prdm1*^{CD} and *prdm1*^{BEH} alleles were intercrossed, we found that the trans-heterozygotes were indistinguishable from *prdm1*^{BEH}, *prdm1*^{BAH} and *prdm1*^{CD} homozygous embryos. These results strongly suggest that our *prmd1*^{BEH} and *prdm1*^{BAH} targeted alleles create loss-of-function mutations.

Blimp1 functional loss causes branchial arch defects

Blimp1 is expressed in the anterior definitive endoderm, with higher levels detected in the lateral region that subsequently gives rise to the branchial arches (Fig. 3A,B). In mammalian embryos, the six pairs of branchial arches develop in a cranial to caudal sequence. In the mouse, the first branchial arch, the precursor of the maxilla and mandible, becomes morphologically apparent at 8.5 dpc, with the second and third arches emerging over the course of the next 24 hours. At 9.5 dpc, *Blimp1* transcripts are restricted to the endodermal layer of the proximal-most region, or cleft, of the first branchial arch (Fig. 3C,D), whereas, by contrast, expression expands into the endoderm, ectoderm and mesenchyme of the more caudally situated second and third arches (Fig. 3C,E). Interestingly *Blimp1* expression is transient, and from 10.5 dpc onwards is barely detectable in pharyngeal tissues (Fig. 3F,G).

Blimp1-deficient embryos are readily identified at 9.5 dpc by their relatively small size and the presence of a unique first branchial arch rather than the three arches observed in wild-type littermates (Fig. 3H, compare with 3K). One of the main components of branchial arch mesenchyme is cranial neural crest. In zebrafish, *ubo* is expressed at the boundary of the neural plate and the non-neural ectoderm at the site where neural crest cells later originate, and loss of *ubo* activity impairs specification of the neural crest cells (Roy and Ng, 2004). In the mouse embryo, *Blimp1* transcripts are not detected in the neural plate nor in migrating neural crest cells (Fig. 3, data not shown), and to evaluate the possibility that the branchial arch defects are caused by aberrant neural crest formation, we assessed expression of the neural crest marker *Crabp1* (Dolle et al., 1989). At 9.0 dpc, mutant and control embryos show no differences in *Crabp1* expression (data not shown). Thus we conclude that loss of *Blimp1* fails to perturb specification and migration of the neural crest cells. Rather, histological analysis reveals that the defect is caused by selective cell death of mesenchyme cells specifically at the site where the second and third arches normally emerge within the strongest *Blimp1* expression domain (Fig. 3K, part 2). The

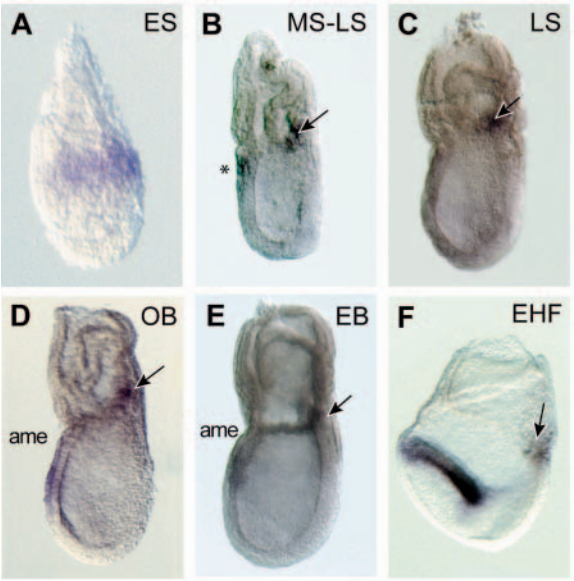

Fig. 1. *Blimp1* expression in the early mouse embryo. Whole-mount in situ hybridization identifies *Blimp1* expression domains at (A) early streak, (B) mid-late streak, (C) late streak, (D) no allantoic bud, (E) early allantoic bud and (F) early headfold stages. (A) In the pre-gastrulation embryo, *Blimp1* is expressed in a sub-population of visceral endoderm overlying the proximal epiblast. (B,C) At mid- to late streak stage, *Blimp1* is detected in the anterior visceral endoderm (AVE, asterisk), and in the nascent primordial germ cells (PGCs) present in the incipient allantois (arrow). (D,E) At later stages, *Blimp1* transcripts mark the prechordal plate and anterior definitive endoderm [labeled collectively as anterior axial mesendoderm (ame)], and PGCs present in the growing proximal posterior extraembryonic mesoderm (arrow). (F) At the early headfold stage (EHF), expression is lost from the midline but persists in the anterior definitive endoderm of the foregut pocket, and within the cluster of individual PGCs at the base of the allantois (arrow). ES, early streak; MS, mid streak; LS, late streak; OB, no allantoic bud; EB, early allantoic bud stages. Embryos are shown anterior to the left.

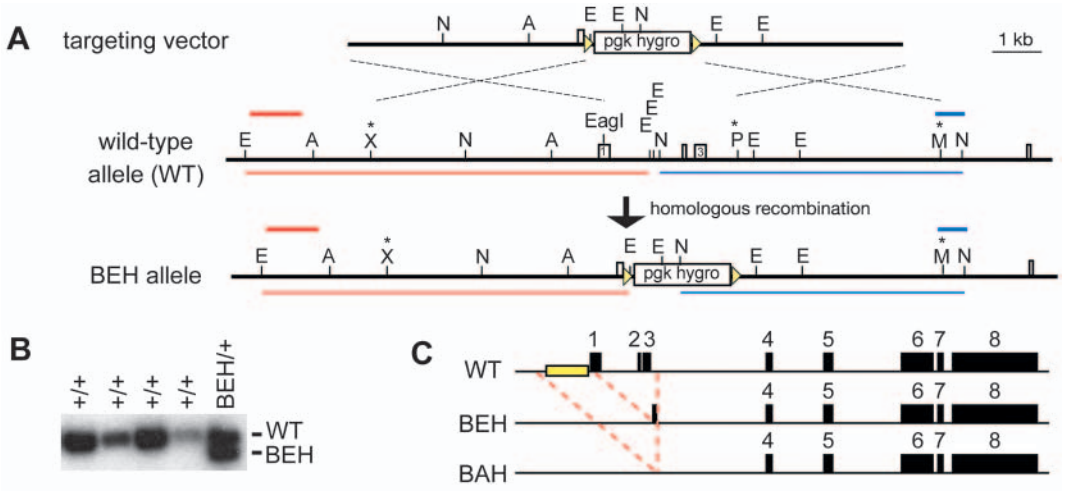

Fig. 2. Generation of loss-of-function *Blimp1* mutants by gene targeting. (A) Strategy used to engineer the *prdm1*^{BEH} allele. Correctly targeted clones were initially identified with the 5′ external probe (red) and subsequently confirmed with the 3′ external probe (blue). A, *Apa*I; E, *Eco*RI; M, *Msc*I; N, *Nco*I; P, *Pst*I; X, *Xba*I. (B) Southern blot analysis of *Eco*RI-digested genomic DNA from individual drug-resistant ES cell clones. The 5′ external probe detects 8.2-kb wild-type (WT) and 7.9-kb targeted *prdm1*^{BEH} alleles. (C) A similar targeting strategy was used to generate the *prdm1*^{BAH} allele, containing an additional 1-kb deletion immediately 5′ to exon 1 (see Materials and methods). The selection cassette is not shown.

presence of apoptotic cells was confirmed by TUNEL analysis (data not shown). In addition, *Fgf8* transcripts, normally co-expressed with *Blimp1* in the endoderm and ectoderm of the emerging caudal second and third arches, are significantly reduced (Fig. 3I-M). By contrast, *Fgf8* expression in the cleft of the first arch is robustly maintained (Fig. 3J,M).

Specification of the myotome and limb bud patterning is unperturbed in *Blimp1* mutant embryos

Blimp1 shows a dynamic pattern of expression from 9.5 dpc onwards. Interestingly, *Blimp1* is expressed at the site where myogenesis is initiated in the myotome of the most rostral somites (reviewed by Tajbakhsh and Buckingham, 2000) (Fig. 4A). As the more caudal somites mature, *Blimp1* expression is detected in the myotomal fibers along the rostrocaudal axis (Fig. 4B,C), and by 11.5 dpc becomes restricted to the myotome of the most caudal somites (Fig. 4D). Expression is confined to the intercalated mytome, located between the most epaxial and hypaxial domains, where muscular differentiation is initiated (Cheng et al., 2004; Spörle, 2001). *Blimp1*-deficient embryos die at 10.5 dpc, precluding our ability to investigate its functional role in the myogenic lineage. However, the expanded *Fgf8* domain in the epaxial dermomyotomal lip of *Blimp1*-deficient embryos suggests a potential role for *Blimp1* in regulation of the myogenic program in mouse (Fig. 3J,M).

Blimp1 transcripts are present throughout the limb bud as it emerges from the flank (Fig. 4A). By E10.5, expression shifts to demarcate the posterior region of the bud (Fig. 4D), encompassing the zone of polarizing activity (ZPA). Interestingly at 10.5 dpc, *Blimp1* expression is also restricted to the distal part of the bud, in a domain that includes the apical ectodermal ridge AER (Fig. 4B,D, and data not shown). These signaling centers control anteroposterior and proximodistal patterning of the growing limb bud, respectively (reviewed by Tickle, 2003). However AER and ZPA patterning proceeds normally in *Blimp1* mutant embryos. Moreover *Fgf8* expression in the AER is unaffected (Fig. 3I-M), strongly suggesting that *Blimp1* does not lie upstream of *Fgf8*. Similarly, the ZPA marker *Shh* shows delayed onset of expression, which is likely to be due to growth retardation of the mutant embryos, but by 10.5 dpc anteroposterior polarity is correctly established, as judged by induction of *Shh* expression (data not shown). The otic vesicle, a tissue showing very strong *Blimp1* expression (Fig. 3C,F) also forms normally (Fig. 3K, part 2).

Table 1. *Blimp1* deficiency results in embryonic death at mid-gestation

	Genotype*			
Age	+/+	+/–	–/–	Total
7.5 dpc	8	20	11† (28%)	39
9.5 dpc	39	96	38‡ (22%)	173
10.5 dpc	18	40	16§ (22%)	74
11.5 dpc	8	18	0 (0%)	26
12.5 dpc	2	4	0 (0%)	6
Neonates	61	93	0 (0%)	154

*No differences were observed between *prdm1*$^{BAH/+}$ and *prdm1*$^{BEH/+}$ intercrosses (see Materials and methods).
†No visible phenotype.
‡Growth retarded, branchial arch defect, heart beating normally.
§Severely growth retarded and hemorrhagic.

Embryonic lethality is associated with severe hemorrhage and placental defects

The major vascular structures of the early embryo, including the dorsal aorta and the yolk sac vasculature form normally in *Blimp1* mutant embryos (Fig. 4). By 9.5 dpc, the heart tube displays correct patterning, and has undergone normal looping morphogenesis (Fig. 4G, compare with 4F) and contracts rhythmically. Histological analysis shows appropriate formation of the myocardial and endocardial cell populations. However, one day later, mutant embryos show widespread apoptosis and become severely hemorrhagic, with blood pooling in the heart, dorsal aorta and under the surface ectoderm (Fig. 5G). We wondered whether the reduced growth rate and mid-gestation lethality might be caused by a placental defect.

Formation of the placenta is a complex process involving sequential interactions of the allantois and the chorionic plate

with the trophoblast derivatives (reviewed by Rossant and Cross, 2002). Around 10.5 dpc, embryonic blood vessels arising from the allantois undergo extensive villus branching within the placenta to create a densely packed network of blood-filled spaces termed the labyrinth, which functions as an exchange zone between maternal and embryonic circulation. Histological analysis shows that these specialized cell types initially develop normally (Fig. 5B,D). However, the labyrinthine region fails to expand correctly, thereby greatly reducing the volume of the blood spaces (Fig. 5D,H; compare with 5B,F, respectively). Whole-mount in situ hybridization experiments failed to demonstrate *Blimp1* transcripts in the extra-embryonic structures that contribute to the placenta, excluding a cell-autonomous defect.

The major blood vessels did not display any obvious abnormalities prior to 10.5 dpc (Fig. 4). At 10.5 and 11.5 dpc,

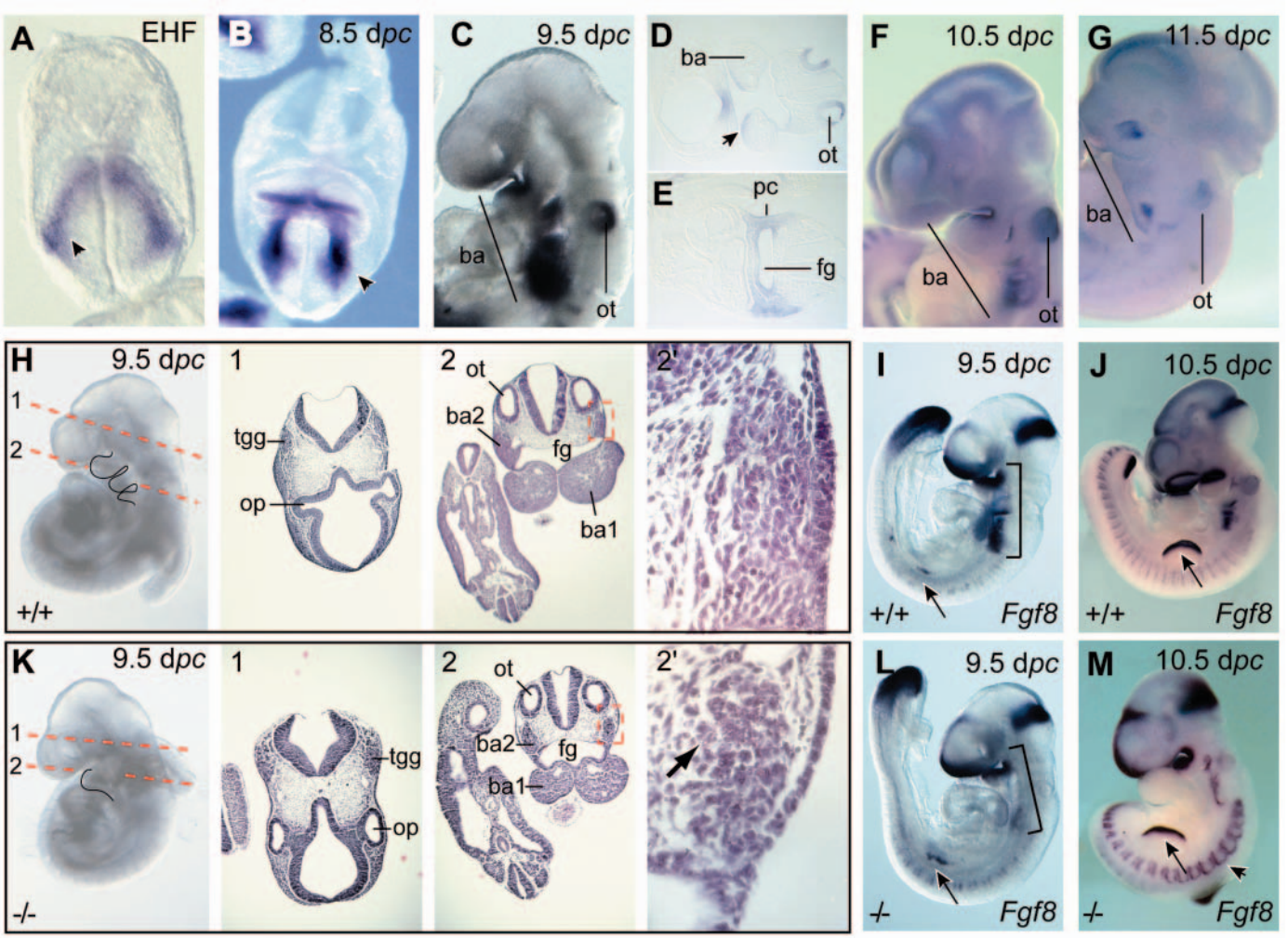

Fig. 3. Loss of *Blimp1* expression causes branchial arch patterning defects. Whole-mount in situ hybridization analysis of *Blimp1* expression in wild-type embryos at (A) 7.75, (B) 8.5, (C) 9.5, (F) 10.5 and (G) 11.5 dpc. (A) *Blimp1* transcripts are expressed in the anterolateral definitive endoderm, most abundantly in the tissue from which the first branchial arch (ba) will emerge (arrowhead). (B) This expression domain is maintained one day later (arrowhead), when *Blimp1* transcripts also appear in the ventral anterior neurectoderm. (C) At 9.5 dpc, *Blimp1* is expressed in the ventral forebrain, and in the regions of the first, second and third branchial arches. (D,E) Transverse sections of embryo shown in C showing expression confined to the pharyngeal endoderm of the first branchial arch (arrow in D), while *Blimp1* is broadly expressed in the ectoderm, mesoderm and endoderm, more caudally in the region from which the second and third arches arise. From this stage onwards, *Blimp1* transcripts are also detected in the foregut (fg) and otic vesicles (ot). (F) At 10.5 dpc, expression is downregulated within the branchial arches, and by 11.5 dpc (G), resolves to a subdomain within the first branchial arch. (H,K) Histological analysis of 9.5 dpc wild-type (+/+; H) and mutant (–/–; K) embryos. (H) Whole-mount view of a 9.5 dpc wild-type embryo and corresponding Hematoxylin-Eosin-stained transverse sections 1 and 2 (levels indicated by dashed lines). Three branchial arches are visible (outlined). (K) In a similarly staged mutant embryo, only the first branchial arch is present (outlined). Defects are restricted to the levels of the second branchial arch (K part 2, compare with H part 2). At this site (see high magnification image in K2′), apoptotic cells with pyknotic nuclei (arrow) accumulate within the mesenchyme (compare with H2′). (I,J,L,M) *Fgf8* expression domains at 9.5 and 10.5 dpc. In 9.5-10.5 dpc embryos, *Fgf8* is expressed at multiple tissue sites, including the ectoderm and endoderm of the branchial arches, the midbrain-hindbrain junction, the somites, the developing limb buds (arrows) and the tail bud. The branchial arch domain in the region of the second and third arches is largely missing in mutant embryos (compare brackets in I and L). (J,M) At 10.5 dpc, *Fgf8* expression is more broadly expressed in the mutant than in the wild type, and extends into the epaxial lip of the rostral dermamyotome (short arrow). *Fgf8* expression at all other sites, including the AER of the limb buds (arrow), is unperturbed. ba, branchial arch; ot, otic vesicle; pc, pharyngeal cleft; fg, foregut; tgg, trigeminal ganglia; op, optic vesicle.

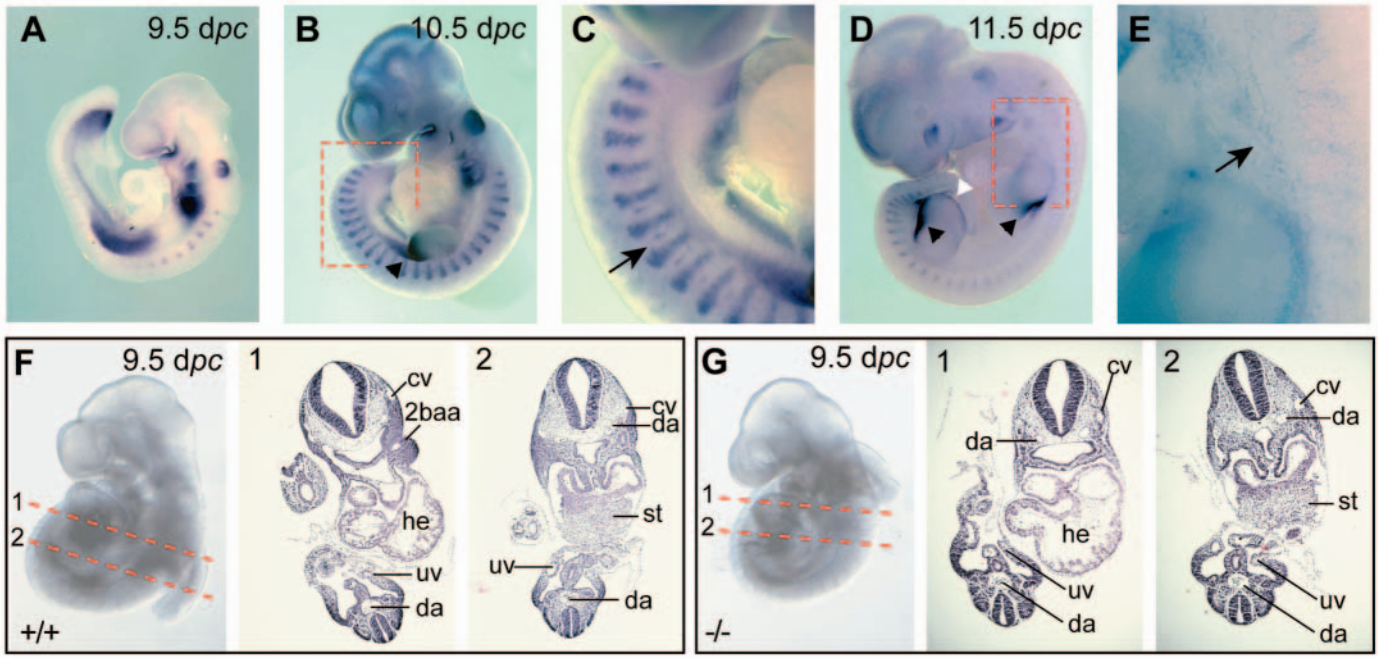

Fig. 4. Morphogenesis and tissue patterning are largely unaffected in *Blimp1*-deficient embryos. Whole-mount in situ hybridization analysis of *Blimp1* expression at (A) 9.5, (B,C) 10.5 and (D,E) 11.5 dpc. (A-D) *Blimp1* mRNA is strongly expressed throughout the mesenchyme of the emerging forelimb bud at 9.5 dpc (A), but becomes progressively restricted to the apical ectodermal ridge (indicated by the white arrowhead in D) and underlying mesenchyme by 10.5 dpc (B). One day later (D), at 11.5 dpc, expression is confined to the posterior side of the limb bud in a region encompassing the zone of polarizing activiy (ZPA, black arrowhead). At 10.5 dpc (B,C), *Blimp1* transcripts are also expressed in the myotomal compartment of the somites, and in the intersegmentary arteries (arrow in C) forming between the somites. At 11.5 dpc (D,E), expression is detected in the endothelial cells of the capillary plexus (arrow in E). *Blimp1* is not expressed in the developing heart at any stage examined. (F,G) Histological analysis of wild-type (+/+) and mutant (–/–) embryos fails to reveal differences in overall morphogenesis and patterning of the heart at 10.5 dpc. (F parts 1 and 2, G parts 1 and 2) Hematoxylin-Eosin stained transverse sections of embryos shown in F and G; planes of section indicated by the red dashed lines. ba, branchial arch; he, heart; st, septum transversum; da, dorsal aorta; cv, anterior cardinal vein; uv, umbilical vein; 2baa, second branchial arch artery.

Blimp1 transcripts are detectable in the developing intersegmentary arteries and the endothelial cells of the superficial capillary plexus (Fig. 4C,E). PECAM staining of endothelial cells throughout the circulatory network of mutant embryos was unperturbed as assessed by whole mount immunohistochemistry (data not shown). Thus it appears that endothelial cells initially form in *Blimp1* mutants, but that the rapid expansion of this cell population necessary to support embryonic growth is compromised. Alternatively, the loss of the caudal branchial arches, which prevents formation of the second and third pharyngeal arteries (Fig. 5C), may secondarily disrupt blood circulation. Conditional deletion of *Blimp1* within the endothelial cell lineages is required to distinguish these possibilities.

Blimp1 is required for specification of primordial germ cells

Around 7.0 dpc, *Blimp1* expression identifies committed PGCs as they first appear at the base of the incipient allantois (Fig. 1B). Expression persists in PGCs as they proliferate and migrate anteriorly along the hindgut toward the genital ridges (Chang and Calame, 2002). To evaluate whether *Blimp1* is required for specification and/or maintenance of the mammalian germ line, we compared PGC numbers in wild-type, heterozygous and homozygous mutant embryos. PGCs are easily identified due to their high endogenous levels of alkaline phosphatase (AP) activity (Ginsburg et al., 1990; Lawson and Hage, 1994). Intercross embryos were collected around 9.0-9.5 dpc. In *Blimp1* null mutant embryos (n=12), we failed to observe AP-positive PGCs, and the number of PGCs in similarly staged heterozygous embryos (n=58) was significantly reduced, when compared with wild type (n=34) (Fig. 6B). These results were confirmed by immunohistochemical staining with the SSEA1 monoclonal antibody (Gomperts et al., 1994). We failed to detect any migrating PGCs within the hindgut epithelium of *Blimp1* mutant embryos, and there were reduced numbers of SSEA1-positive PGCs in heterozygotes, when compared with wild type (Fig. 6C).

To determine the onset of the PGC phenotype, embryos were collected and stained for AP activity between 8.0 and 9.5 dpc. The number of PGCs was plotted against somite number and the regression line of the log PGC number calculated. Extrapolation of the regression lines gives a founding population of 40 PGCs in wild type (Fig. 7), consistent with previous estimates of approximately 45 founder cells (Lawson and Hage, 1994). By contrast, a founding population of nine was observed for *Blimp1* heterozygotes (a reduction of 78%), revealing strong gene-dosage sensitivity. The slopes of the regression lines are not significantly different, indicating that both wild type and *Blimp1* heterozygous PGCs expand at similar rates. Furthermore, we observed no differences in the

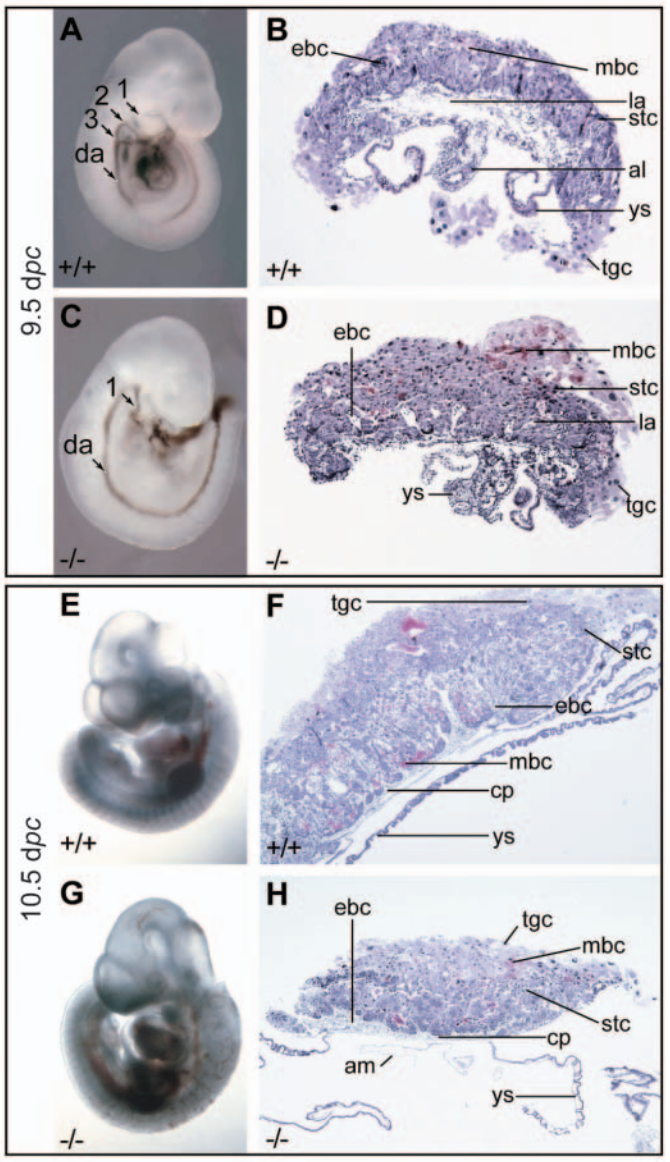

Fig. 5. Widespread hemorrhaging and defective placental development in *Blimp1* mutant embryos. (A,C) The heart is still beating in 9.5 dpc mutant embryos, and injection of India ink into the outflow tract outlines the major arterial system. The dorsal aorta is visible in both wild-type (A) and mutant (C) embryos. Compared with wild type, only the first branchial arch artery (1) is visible in the mutant. (G) By 10.5 dpc, *Blimp1*-deficient embryos show widespread hemorrhaging. Numerous small blood pools form beneath the surface ectoderm and blood accumulates in the caudal dorsal aorta. (B,D,F,H) Hematoxylin-Eosin-stained mid-sagittal sections of wild-type (B,F) and mutant (D,H) placentas at 9.5 and 10.5 dpc. At 9.5 dpc (B,D), all the major tissue components of the wild-type placenta (B) have differentiated correctly. However, at this stage, the mutant placenta (D) displays defects in elaboration of the labyrinthine region; the luminal spaces of the labyrinth are much reduced when compared with the wild type. This defect is further exacerbated 24 hours later (H), when very little villous branching of the fetal blood vessels is apparent. Both maternal and embryonic erythrocytes are present. ebc, embryonic blood cells; mbc, maternal blood cells; stc, spongiotrophoblast; la, labyrinthine; tgc, trophoblast giant cells; ys, yolk sac; al, allantois; cp, chorionic plate; am, amnion; da, dorsal aorta; 1, first branchial arch; 2, second branchial arch; 3, third branchial arch.

regional distribution of PGCs along the hindgut epithelium (Fig. 5B). Thus *Blimp1* is required for initial PGC specification.

To strengthen this interpretation, we evaluated PGC numbers soon after they first appear (Downs and Davies, 1993; Lawson and Hage, 1994). At the headfold stage (7.75 dpc), PGCs begin to disperse from the base of the allantois and intercalate into the forming hindgut. We observed reduced numbers of PGCs in *Blimp1* mutant heterozygotes, when compared with wild type (Fig. 6A), whereas in homozygous mutants (n=6) fewer than two to four AP-positive cells were present, or PGCs were undetectable (Fig. 6A). AP-positive cells thus fail to survive (Fig. 6B,C). We conclude that *Blimp1* functions to promote the formation of nascent PGCs.

Discussion

Here we demonstrate, contrary to expectations from studies in *Xenopus* and zebrafish, that *Blimp1* is not required for establishment of the anteroposterior axis in early mouse embryos. These results are especially surprising because *Blimp1* is expressed at the right time and place to influence formation of head structures, namely in axial mesendoderm, the tissue known to provide anterior patterning signals during gastrulation. *Blimp1* is not expressed specifically in the AVE but rather is induced in a ring of visceral endoderm at the embryonic/extra-embryonic junction. Loss of highly transient *Blimp1* expression in the visceral endoderm has no effect on early post-implantation development. *Blimp1* transcripts are broadly and dynamically expressed at later stages, but surprisingly mutant embryos display quite restricted tissue defects.

The identical phenotype results from two independent targeting strategies that deleted different regions of the locus. Heart development per se proceeds normally, but at around 10.5 dpc, we observe blood leakage from the superficial capillaries, and accumulation of blood within the heart and dorsal aorta. Mutations causing hemorrhaging phenotypes have been extensively described in the various signaling pathways that control endothelial cell function and formation (reviewed by Sato and Loughna, 2002). Our experiments demonstrate that *Blimp1* is expressed in the endothelium and intersegmental arteries. Specification of endothelial cells proceeds normally, as assessed by histological examination and PECAM expression, suggesting that *Blimp1* is not required during formation of the vasculature but probably acts later to regulate angiogenesis and/or vascular remodeling. It will be interesting to test this possibility in conditional mutants selectively lacking *Blimp1* in the endothelium.

The growth retardation and rapid death of the *Blimp1*-deficient embryos is most likely due to placental insufficiency. All of the specialized placental cell types are correctly specified in *Blimp1* mutant embryos. However the labyrinth region, the site of major maternal/fetal exchange, is poorly developed at 9.5 dpc, and by 10.5 dpc, mutant placentas display striking morphogenetic defects coincident with rapid growth of the embryo. At this stage the essential nutrient and oxygen exchange functions provided by the visceral yolk sac normally shift to the mature placenta. *Blimp1* transcripts are undetectable in the placenta, suggesting the labyrinth defects arise as a secondary consequence of abnormalities restricted to

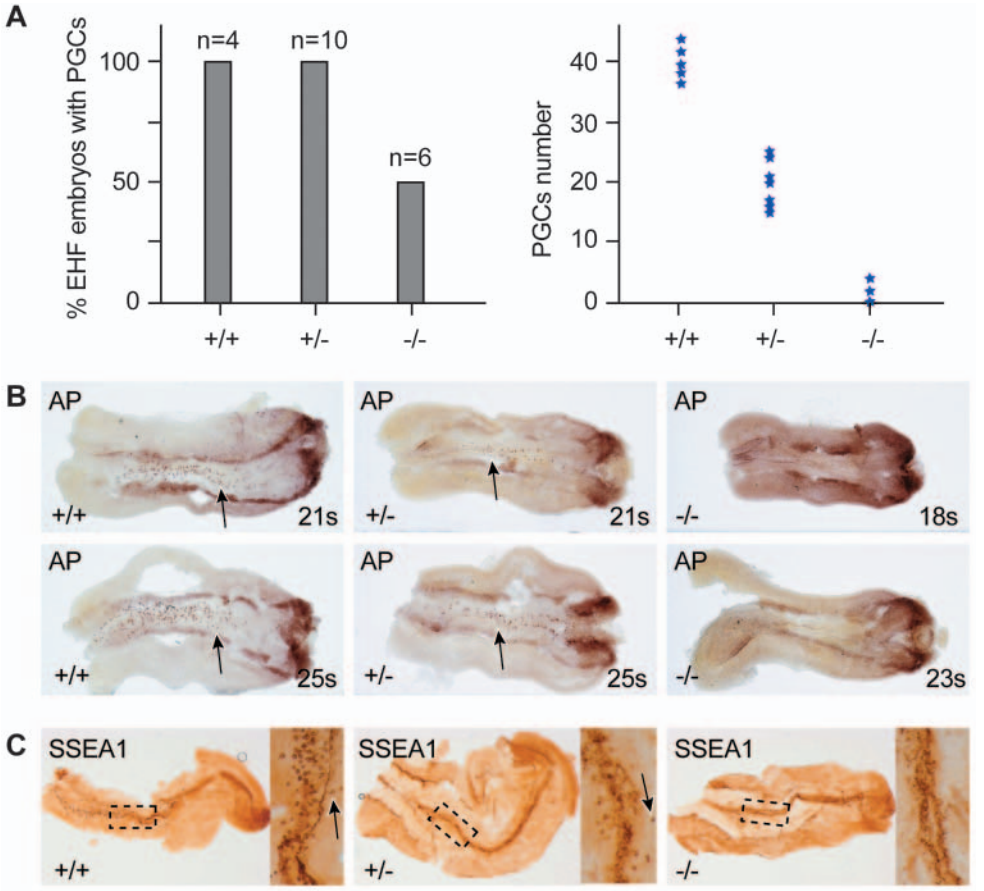

Fig. 6. Defective specification of primordial germ cells (PGCs) in *Blimp1* mutant embryos. Endogenous alkaline phosphatase (AP) activity and SSEA1 antibody reactivity identifies PGCs. (A) Number of embryos in which AP-positive PGCs could be identified at the early headfold stage (EHF). Genotypes are indicated. Cell counts show that *Blimp1* heterozygotes display less than 50% of the wild-type number of PGCs, while less than four AP-positive PGCs were observed in three out of six *Blimp1* homozygous mutants. (B) AP staining in wild-type (+/+), heterozygous (+/–) and homozygous (–/–) mutants at the indicated somite (s) stage. Reduced PGC numbers were found in the heterozygotes (arrow) compared with the wild-type siblings, and no migrating PGCs were detected in homozygous mutants embryos. (C) Evaluation of individual SSEA1 cell-surface-antigen-positive cells in the hindgut of wild-type (+/+), heterozygous (+/–) and homozygous (–/–) mutants confirms the absence of migrating PGCs in *Blimp1* null embryos, and reveals that significantly fewer SSEA1-positive cells are present in heterozygotes than in controls. Midline staining corresponds to SSEA1 reactivity with the hindgut lumen.

the embryonic vasculature. The importance of blood flow in shaping the vasculature is well documented. Reduced blood flow due to hemorrhage thus potentially disrupts the mechanical signals necessary for villous branching in the placental labyrinth.

Organogenesis and tissue patterning are largely unaffected. However, *Blimp1*-deficient embryos display striking branchial arch defects. The branchial arches form from four distinct cell subpopulations. The core, comprising lateral mesenchymal cells and neural crest cells, interacts with the adjacent endoderm and surface ectoderm tissues. *Blimp1* is expressed in the dorsal anterior regions of the emerging branchial arches, specifically in the pharyngeal endoderm. In the first arch, *Blimp1* transcripts are only present in the endoderm, whereas in the second and third arch expression is more widespread, extending into the mesenchyme. Formation of the second and third arches correctly initiates around 9.5 dpc, but in *Blimp1* mutant embryos these structures deteriorate shortly thereafter. Reduced *Blimp1* activity in the hypomorphic zebrafish mutant *ubo* similarly leads to pectoral fin defects, implicating an evolutionarily conserved role for *Blimp1* in patterning branchial arch derivatives (van Eeden et al., 1996).

In fish, BMP signals induce *Blimp1* expression at the boundary between neural and non-neural ectoderm, which in turn promotes formation of neural crest and sensory neuron progenitors (Roy and Ng, 2004). However, the caudal branchial arch defects described here cannot be explained as a deficiency in neural crest because *Crabp1* expression in *Blimp1* mutant embryos is unperturbed. Thus, neural crest cells are correctly specified and efficiently migrate into the forming arches. Rather, branchial arch defects closely resemble those caused by reduced Fgf signaling. *Fgf8* is expressed in both the branchial arch ectoderm and endoderm, and is required for survival of the neural crest. Localized cell death has been observed in the branchial arches of *Fgf8* hypomorphs and conditional mutants (Abu-Issa et al., 2002; Frank et al., 2002; Macatee et al., 2003; Trumpp et al., 1999). *Blimp1* mutants similarly display numerous apoptotic cells with pyknotic nuclei in caudal branchial arches. These results suggest that *Blimp1* positively regulates *Fgf8* in the pharyngeal endoderm. The pharyngeal endoderm is thought to play a crucial role in coordinating branchial arch outgrowth (reviewed by Graham, 2003; Graham et al., 2004). Cell death in the arches probably compromises continued arch outgrowth, and disrupts the survival or mitogenic cues necessary to create a permissive environment for incoming neural crest and paraxial mesenchyme.

Interestingly these defects are restricted to branchial arches 2 and 3, whereas the first arch develops normally, a phenotype reminiscent of the *Raldh2* mutants and those rescued by maternal retinoic acid (RA) supplementation (Niederreither et al., 1999; Niederreither et al., 2003). Expression of the RA-responsive genes *Hoxa1* and *Hoxb1*, normally present in the foregut endoderm, is entirely absent in *Raldh2* mutants, and these transcripts are expressed at reduced levels in the rescued embryos. Interestingly, the first arch does not express either of these Hox genes. By contrast, formation of the posterior arches is sensitive to fluctuating Hox levels (Rijli et al., 1993; Rossel

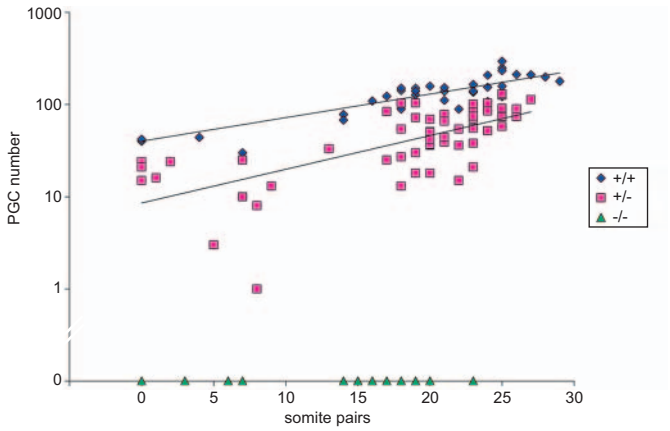

Fig. 7. Linear regression analysis of PGC numbers versus somite numbers in embryos from *Blimp1* heterozygous intercrosses. Combined PGC counts from *prdm1*$^{BEH/+}$ and *prdm1*$^{BAH/+}$ (C57BL/6×129/Sv//Ev) intercrosses. The values in the regression equation $y=a+bx$, for log PGC number (y) and somite number (x) were a=1.603 and b=0.0587, and a=0.9324 and b=0.0842, for wild type and *Blimp1* heterozygotes, respectively. The variances between PGC number and somite number are not significantly different according to the F test ($F=2.2\times10^{-22}$ and $F=5.4\times10^{-23}$ for wild type and heterozygotes, respectively).

and Capecchi, 1999). Here, we observe that *Blimp1* is co-expressed with *Hoxa1/Hoxb1* in the foregut endoderm. An attractive idea is that the focal defects in arch formation reflect selective *Blimp1* requirements upstream of Hox gene expression. It will be interesting to learn more about *Blimp1* targets in the branchial arches and the extent to which these pathways overlap with those governing terminal B cell differentiation and germ cell specification.

Here, we demonstrate for the first time that the zinc-finger transcriptional repressor *Blimp1* is required for specification of the mammalian germ line. *Blimp1* transcripts appear to tightly localize to PGCs, coincident with their emergence in the extra-embryonic mesoderm. *Blimp1* is initially expressed in a subpopulation of VE overlying the proximal region of the epiblast adjacent to the distal extra-embryonic ectoderm. It is well known that Bmp4 plays an essential role during germ-cell specification. Bmp4 signals from the extra-embryonic ectoderm (Lawson et al., 1999), together with Alk2, which is expressed in the VE (de Sousa Lopes et al., 2004), and the intracellular effectors Smad1, Smad5 and Smad4 (Chang and Matzuk, 2001; Chu et al., 2004; Tremblay et al., 2001) are required to promote both germ cell and posterior mesoderm/allantoic fates in a dose-dependent fashion. As for neural crest progenitors in zebrafish (Roy and Ng, 2004), we suggest that the Bmp4 pathway also governs *Blimp1* induction during germ-cell specification. Relatively little is known about transcriptional control at the *Blimp1* locus, but we speculate that *Blimp1* expression in PGCs in part depends on Bmp4 signals acting upstream of Smad effector proteins. Consistent with this idea Smad1, Smad5 and Smad4 mutant embryos display germ-cell defects (Chang and Matzuk, 2001; Chu et al., 2004; Tremblay et al., 2001).

A recent screen identified two candidate genes potentially involved in the establishment of germ-cell competence in the proximal epiblast (Saitou et al., 2002). Fragilis/Ifitm3, an interferon-inducible transmembrane protein, is broadly induced in proximal epiblast cells adjacent to the extra-embryonic ectoderm (Tanaka and Matsui, 2002; Tanaka et al., 2004), and is activated in response to Bmp4 signaling in a dose-dependent fashion. Expression rapidly resolves to the proximal posterior side of the embryo, and becomes confined to the PGCs, but its functional role in germ-cell specification has yet to be characterized. The gene *stella* (*Dppa3* – Mouse Genome Informatics), encodes a novel intracellular protein, activated later within the PGCs, that is nonessential for germ-cell specification (Payer et al., 2003; Bortvin et al., 2004). It has been proposed that genes such as fragilis and stella act to turn off genes that promote somatic cell fates, including transcription factors such as *Hoxb1* and *Evx1*, and thus create a niche for PGC specification (Saitou et al., 2002).

The present data suggests that *Blimp1* turns off the default pathway that allows epiblast cells to adopt a somatic cell fate and shifts the transcriptional profile so that *Blimp1*-expressing cells become exclusively allocated into the germ-cell lineage. Germ-cell specification involves the repression of region-specific homeobox genes such as *Hoxa1/Hoxb1*, *Lim1* and *Evx1* in adjacent somatic cells. *Evx1* and *Hoxb1* expression domains were not expanded in *Blimp1*-deficient embryos (data not shown), but this might reflect our inability to assess expression at single-cell resolution via WISH. Interestingly, we observe pronounced dose-dependent *Blimp1* requirements, which suggests that a relatively high threshold of *Blimp1* activity is required for germ-cell differentiation and survival. An important future goal is the identification of *Blimp1* targets downstream in the molecular program responsible for specification of germ cells.

In Xenopus, *Blimp1* activates *Cerberus* expression and antagonizes TGFβ and Wnt signals (de Souza et al., 1999). However TGFβ antagonists play more a subtle role in axis patterning in mouse embryos. Indeed, mutants lacking *cerberus* (*Cer1* – Mouse Genome Informatics) are viable, most likely as a result of redundancy in these signaling pathways. Cerberus activities in mice were only uncovered in double-mutant embryos also lacking *Lefty1*, a second TGFβ family antagonist (Perea-Gomez et al., 2002). Cerberus is thus also a candidate *Blimp1* target in early mouse embryos.

Blimp1 contains five consecutive Krüppel-type zinc fingers in the C-terminal region, and a positive-regulatory (PR) domain at the N terminus that is necessary for chromatin remodeling. The middle proline-rich region recruits members of the Groucho family of co-repressors and members of the histone deacetylase families (Ren et al., 1999; Yu et al., 2000). These various functional modules coordinate the ability of *Blimp1* to function as a master regulator of gene expression. Considerable evidence suggests that *Blimp1* acts as a DNA-binding scaffold protein capable of directly recruiting multiple chromatin-modifying enzymes to targeted promoters. The molecular mechanisms underlying *Blimp1* activities during plasma cell differentiation have been extensively characterized. As a master regulator of the B-cell lineage, *Blimp1* functions upstream of transcription factors such as CTIIA and Pax5, which govern antigen presentation and receptor signaling (Lin et al., 2002; Piskurich et al., 2000). *Blimp1* also represses genes, such as *Myc*, which are involved in cell cycle progression (Lin et al., 1997). In contrast, *Blimp1* activates expression of XBP, a transcription factor in the unfolded-

protein-response pathway that is required for plasma cell differentiation (Lin et al., 2002; Shaffer et al., 2002; Shapiro-Shelef et al., 2003). The present study demonstrates that *Blimp1* is an essential regulator of branchial arch formation and germ cell specification. Future experiments aim to characterize how *Blimp1* promotes programmed differentiation and/or survival of these distinct cell types in the developing mammalian embryo.

We thank Debbie Pelusi for help with genotyping. S.D.V. was supported by a Long Term Fellowship from the Human Frontier Science Program Organization (HFSPO). N.R.D. was supported by a postdoctoral fellowship from the NICHD. This work was supported by grants from the NIH and the Wellcome Trust to E.J.R.

References

Abu-Issa, R., Smyth, G., Smoak, I., Yamamura, K. and Meyers, E. N. (2002). Fgf8 is required for pharyngeal arch and cardiovascular development in the mouse. *Development* **129**, 4613-4625.

Baxendale, S., Davison, C., Muxworthy, C., Wolff, C., Ingham, P. W. and Roy, S. (2004). The B-cell maturation factor Blimp-1 specifies vertebrate slow-twitch muscle fiber identity in response to Hedghog signaling. *Nat. Genet.* **36**, 88-93.

Bortvin, A., Goodheart, M., Liao, M. and Page, D. C. (2004). Dppa3 / Pgc7 / stella is a maternal factor and is not required for germ cell specification in mice. *BMC Dev. Biol.* **4**, 2.

Calame, K. L., Lin, K. I. and Tunyaplin, C. (2003). Regulatory mechanisms that determine the development and function of plasma cells. *Annu. Rev. Immunol.* **21**, 205-230.

Chang, D. and Calame, K. (2002). The dynamic expression pattern of B lymphocyte induced maturation protein-1 (Blimp-1) during mouse embryonic development. *Mech. Dev.* **117**, 305-309.

Chang, D. H., Angelin-Duclos, C. and Calame, K. (2000). BLIMP-1: trigger for differentiation of myeloid lineage. *Nat. Immunol.* **1**, 169-176.

Chang, H. and Matzuk, M. M. (2001). Smad5 is required for mouse primordial germ cell development. *Mech. Dev.* **104**, 61-67.

Cheng, L., Alvares, L. E., Ahmed, M. U., El-Hanfy, A. S. and Dietrich, S. (2004). The epaxial-hypaxial subdivision of the avian somite. *Dev. Biol.* **274**, 348-369.

Chu, G. C., Dunn, N. R., Anderson, D. C., Oxburgh, L. and Robertson, E. J. (2004). Differential requirements for Smad4 in TGFbeta-dependent patterning of the early mouse embryo. *Development* **131**, 3501-3512.

de Sousa Lopes, S. M., Roelen, B. A., Monteiro, R. M., Emmens, R., Lin, H. Y., Li, E., Lawson, K. A. and Mummery, C. L. (2004). BMP signaling mediated by ALK2 in the visceral endoderm is necessary for the generation of primordial germ cells in the mouse embryo. *Genes Dev.* **18**, 1838-1849.

de Souza, F. S., Gawantka, V., Gomez, A. P., Delius, H., Ang, S. L. and Niehrs, C. (1999). The zinc finger gene Xblimp1 controls anterior endomesodermal cell fate in Spemann's organizer. *EMBO J.* **18**, 6062-6072.

Dolle, P., Ruberte, E., Kastner, P., Petkovich, M., Stoner, C. M., Gudas, L. J. and Chambon, P. (1989). Differential expression of genes encoding alpha, beta and gamma retinoic acid receptors and CRABP in the developing limbs of the mouse. *Nature* **342**, 702-705.

Downs, K. M. and Davies, T. (1993). Staging of gastrulating mouse embryos by morphological landmarks in the dissecting microscope. *Development* **118**, 1255-1266.

Frank, D. U., Fotheringham, L. K., Brewer, J. A., Muglia, L. J., Tristani-Firouzi, M., Capecchi, M. R. and Moon, A. M. (2002). An Fgf8 mouse mutant phenocopies human 22q11 deletion syndrome. *Development* **129**, 4591-4603.

Ginsburg, M., Snow, M. H. and McLaren, A. (1990). Primordial germ cells in the mouse embryo during gastrulation. *Development* **110**, 521-528.

Gomperts, M., Garcia-Castro, M., Wylie, C. and Heasman, J. (1994). Interactions between primordial germ cells play a role in their migration in mouse embryos. *Development* **120**, 135-141.

Graham, A. (2003). Development of the pharyngeal arches. *Am. J. Med. Genet.* **119A**, 251-256.

Graham, A., Begbie, J. and McGonnell, I. (2004). Significance of the cranial neural crest. *Dev. Dyn.* **229**, 5-13.

Keller, A. D. and Maniatis, T. (1991). Identification and characterization of a novel repressor of beta-interferon gene expression. *Genes Dev.* **5**, 868-879.

Labosky, P. A. and Hogan, B. L. (1999). Mouse primordial germ cells. Isolation and in vitro culture. *Methods Mol. Biol.* **97**, 201-212.

Lawson, K. A. and Hage, W. J. (1994). Clonal analysis of the origin of primordial germ cells in the mouse. *Ciba Found. Symp.* **182**, 68-84; discussion 84-91.

Lawson, K. A., Dunn, N. R., Roelen, B. A., Zeinstra, L. M., Davis, A. M., Wright, C. V., Korving, J. P. and Hogan, B. L. (1999). Bmp4 is required for the generation of primordial germ cells in the mouse embryo. *Genes Dev.* **13**, 424-436.

Lin, K. I., Angelin-Duclos, C., Kuo, T. C. and Calame, K. (2002). Blimp-1-dependent repression of Pax-5 is required for differentiation of B cells to immunoglobulin M-secreting plasma cells. *Mol. Cell. Biol.* **22**, 4771-4780.

Lin, Y., Wong, K. and Calame, K. (1997). Repression of c-myc transcription by Blimp-1, an inducer of terminal B cell differentiation. *Science* **276**, 596-599.

Macatee, T. L., Hammond, B. P., Arenkiel, B. R., Francis, L., Frank, D. U. and Moon, A. M. (2003). Ablation of specific expression domains reveals discrete functions of ectoderm- and endoderm-derived FGF8 during cardiovascular and pharyngeal development. *Development* **130**, 6361-6374.

Nagy, A., Gertsenstein, M., Vintersten, K. and Behringer, R. R. (2003). *Manipulating the Mouse Embryo: a Laboratory Manual.* New York, NY: Cold Spring Harbor Laboratory Press.

Niederreither, K., Subbarayan, V., Dolle, P. and Chambon, P. (1999). Embryonic retinoic acid synthesis is essential for early mouse post-implantation development. *Nat. Genet.* **21**, 444-448.

Niederreither, K., Vermot, J., Le Roux, I., Schuhbaur, B., Chambon, P. and Dolle, P. (2003). The regional pattern of retinoic acid synthesis by RALDH2 is essential for the development of posterior pharyngeal arches and the enteric nervous system. *Development* **130**, 2525-2534.

Payer, B., Saitou, M., Barton, S. C., Thresher, R., Dixon, J. P. C., Zahn, D., Colledge, W. H., Carlon, M. B. L., Nakano, T. and Surani, M. A. (2003). Stella is a maternal effect gene required for normal early development in mouse. *Curr. Biol.* **13**, 2110-2117.

Perea-Gomez, A., Vella, F. D., Shawlot, W., Oulad-Abdelghani, M., Chazaud, C., Meno, C., Pfister, V., Chen, L., Robertson, E., Hamada, H. et al. (2002). Nodal antagonists in the anterior visceral endoderm prevent the formation of multiple primitive streaks. *Dev. Cell* **3**, 745-756.

Piskurich, J. F., Lin, K. I., Lin, Y., Wang, Y., Ting, J. P. and Calame, K. (2000). BLIMP-I mediates extinction of major histocompatibility class II transactivator expression in plasma cells. *Nat. Immunol.* **1**, 526-532.

Ren, B., Chee, K. J., Kim, T. H. and Maniatis, T. (1999). PRDI-BF1/Blimp-1 repression is mediated by corepressors of the Groucho family of proteins. *Genes Dev.* **13**, 125-137.

Rijli, F. M., Mark, M., Lakkaraju, S., Dierich, A., Dolle, P. and Chambon, P. (1993). A homeotic transformation is generated in the rostral branchial region of the head by disruption of Hoxa-2, which acts as a selector gene. *Cell* **75**, 1333-1349.

Rossant, J. and Cross, J. C. (2002). Extraembryonic Lineages. In *Mouse Development: Patterning, Morphogenesis, and Organogenesis* (ed. J. Rossant and P. P. L. Tam), pp. 155-180. San Diego, CA: Academic Press.

Rossel, M. and Capecchi, M. R. (1999). Mice mutant for both Hoxa1 and Hoxb1 show extensive remodeling of the hindbrain and defects in craniofacial development. *Development* **126**, 5027-5040.

Roy, S. and Ng, T. (2004). Blimp-1 specifies neural crest and sensory neuron progenitors in the zebrafish embryo. *Curr. Biol.* **14**, 1772-1777.

Roy, S., Wolff, C. and Ingham, P. W. (2001). The u-boot mutation identifies a Hedgehog-regulated myogenic switch for fiber-type diversification in the zebrafish embryo. *Genes Dev.* **15**, 1563-1576.

Saitou, M., Barton, S. C. and Surani, M. A. (2002). A molecular programme for the specification of germ cell fate in mice. *Nature* **418**, 293-300.

Sato, T. N. and Loughna, S. (2002). Vasculogenesis and Angiogenesis. In *Mouse Development: Patterning, Morphogenesis, and Organogenesis* (ed. J. Rossant and P. P. L. Tam), pp. 211-233. San Diego, CA: Academic Press.

Sciammas, R. and Davis, M. M. (2004). Modular nature of Blimp-1 in the regulation of gene expression during B cell maturation. *J. Immunol.* **172**, 5427-5440.

Shaffer, A. L., Lin, K. I., Kuo, T. C., Yu, X., Hurt, E. M., Rosenwald, A., Giltnane, J. M., Yang, L., Zhao, H., Calame, K. et al. (2002). Blimp-1 orchestrates plasma cell differentiation by extinguishing the mature B cell gene expression program. *Immunity* **17**, 51-62.

Shapiro-Shelef, M., Lin, K. I., McHeyzer-Williams, L. J., Liao, J., McHeyzer-Williams, M. G. and Calame, K. (2003). Blimp-1 is required

for the formation of immunoglobulin secreting plasma cells and pre-plasma memory B cells. *Immunity* **19**, 607-620.

Snedecor, G. W. and Cochran, W. G. (1967). *Statistical Methods*. Ames, IA: Iowa State University Press.

Spörle, R. (2001). Epaxial-adaxial-hypaxial regionalisation of the vertebrate somite: evidence for a somitic organiser and a mirror-image duplication. *Dev. Genes Evol.* **211**, 198-217.

Tajbakhsh, S. and Buckingham, M. (2000). The birth of muscle progenitor cells in the mouse: spatiotemporal considerations. *Curr. Top. Dev. Biol.* **48**, 225-268.

Tanaka, S. S. and Matsui, Y. (2002). Developmentally regulated expression of mil-1 and mil-2, mouse interferon-induced transmembrane protein like genes, during formation and differentiation of primordial germ cells. *Gene Expr. Patt.* **2**, 297-303.

Tanaka, S. S., Nagamatsu, G., Tokitake, Y., Kasa, M., Tam, P. P. and Matsui, Y. (2004). Regulation of expression of mouse interferon-induced transmembrane protein like gene-3, Ifitm3 (mil-1, fragilis), in germ cells. *Dev. Dyn.* **230**, 651-659.

Tickle, C. (2003). Patterning systems – from one end of the limb to the other. *Dev. Cell* **4**, 449-458.

Tremblay, K. D., Dunn, N. R. and Robertson, E. J. (2001). Mouse embryos lacking Smad1 signals display defects in extra-embryonic tissues and germ cell formation. *Development* **128**, 3609-3621.

Trumpp, A., Depew, M. J., Rubenstein, J. L., Bishop, J. M. and Martin, G. R. (1999). Cre-mediated gene inactivation demonstrates that FGF8 is required for cell survival and patterning of the first branchial arch. *Genes Dev.* **13**, 3136-3148.

Turner, C. A., Jr, Mack, D. H. and Davis, M. M. (1994). Blimp-1, a novel zinc finger-containing protein that can drive the maturation of B lymphocytes into immunoglobulin-secreting cells. *Cell* **77**, 297-306.

van Eeden, F. J., Granato, M., Schach, U., Brand, M., Furutani-Seiki, M., Haffter, P., Hammerschmidt, M., Heisenberg, C. P., Jiang, Y. J., Kane, D. A. et al. (1996). Mutations affecting somite formation and patterning in the zebrafish, Danio rerio. *Development* **123**, 153-164.

Vincent, S. D. and Robertson, E. J. (2003). Highly efficient transgene-independent recombination directed by a maternally derived SOX2CRE transgene. *Genesis* **37**, 54-56.

Vincent, S. D., Dunn, N. R., Hayashi, S., Norris, D. P. and Robertson, E. J. (2003). Cell fate decisions within the mouse organizer are governed by graded Nodal signals. *Genes Dev.* **17**, 1646-1662.

Vincent, S. D., Norris, D. P., Ann Le Good, J., Constam, D. B. and Robertson, E. J. (2004). Asymmetric Nodal expression in the mouse is governed by the combinatorial activities of two distinct regulatory elements. *Mech. Dev.* **121**, 1403-1415.

Yu, J., Angelin-Duclos, C., Greenwood, J., Liao, J. and Calame, K. (2000). Transcriptional repression by blimp-1 (PRDI-BF1) involves recruitment of histone deacetylase. *Mol. Cell. Biol.* **20**, 2592-2603.